AtPGAP1 functions as a GPI inositol-deacylase required for efficient transport of GPI-anchored proteins

César Bernat-Silvestre, Judit Sanchez-Simarro, Yingxuan Ma, Javier Montero-Pau, Kim Johnson, Fernando Aniento and María Jesús Marcote

SUPPLEMENTAL MATERIAL

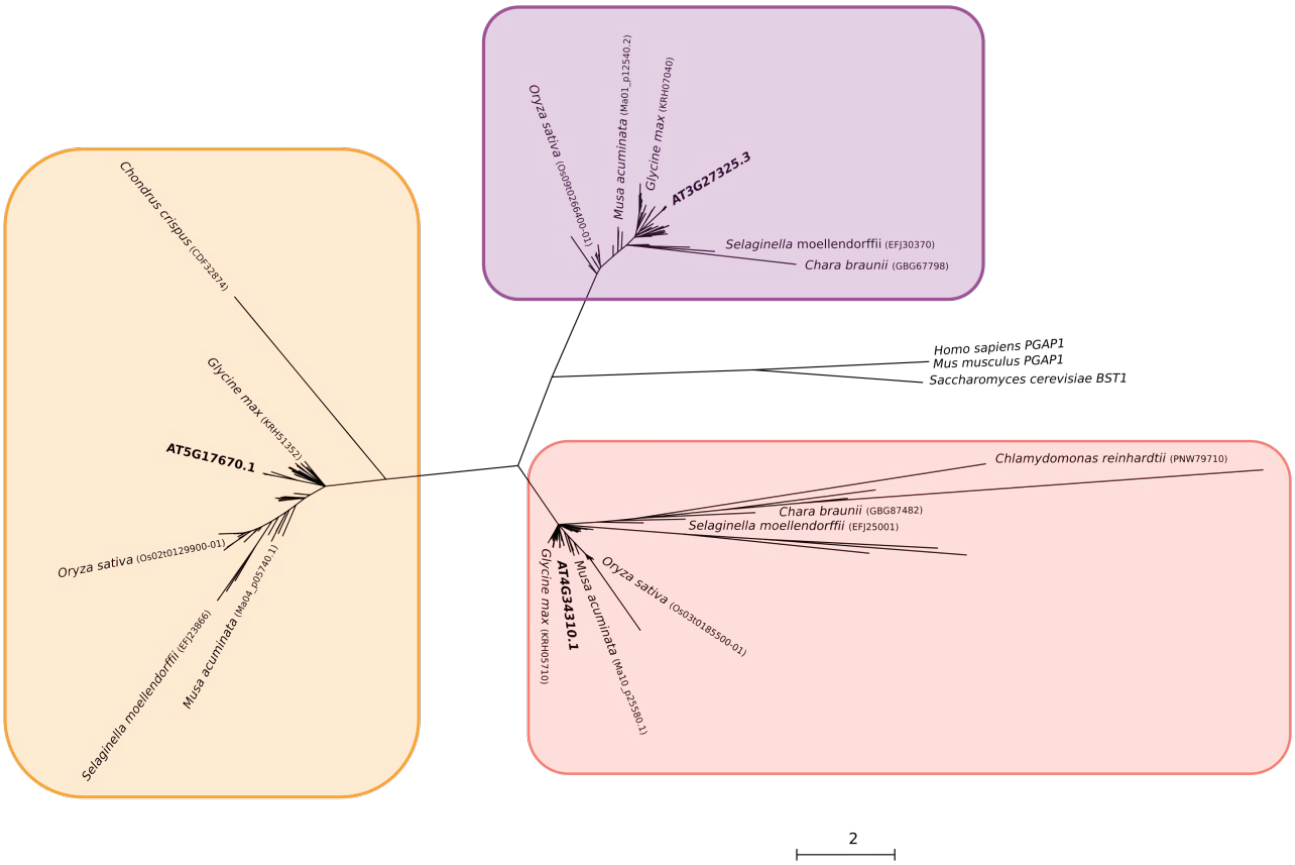

Supplemental Figure S1. Phylogenetic analysis of *PGAP1*-like genes. Maximum-likelihood tree based on 271 protein ortholog sequences of the three *Arabidopsis* genes presenting a complete or partial PGAP1 motif. For clarity purposes, only a few species names are shown. Codes between parentheses correspond to Ensemble Plant IDs. Nodes with a boostrap support lower than 80% have been collapsed.

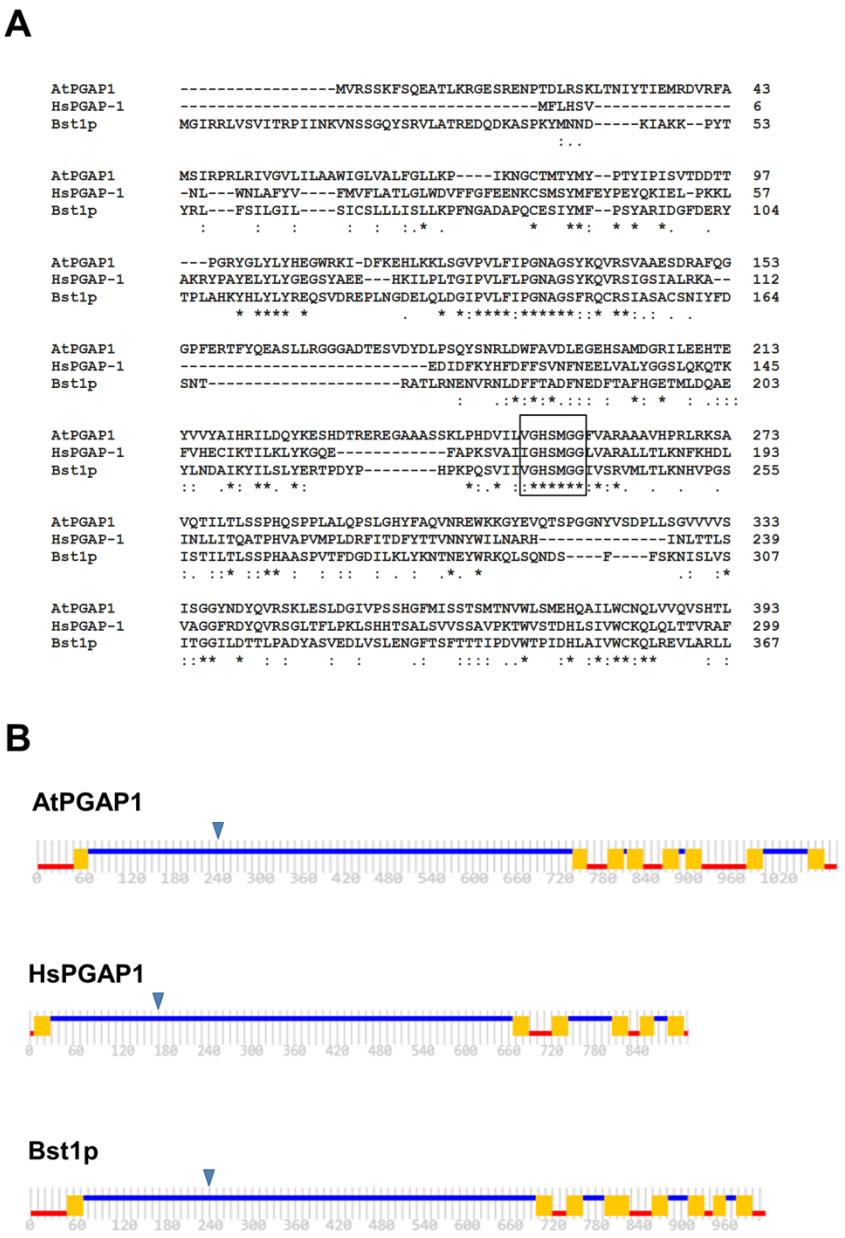

Supplemental Figure S2. Alignment of N-terminal sequences and topology prediction of AtPGAP1, HsPGAP1 and Bst1p. A. Alignment of the N-terminal sequences of AtPGAP1 (At3g27325) (*Arabidopsis thaliana*), HsPGAP1 (*Homo sapiens*) and Bst1p (*Saccharomyces cerevisiae*). The ClustalW software was used. The square shows the lipase consensus domain, including the putative catalytic serine. B. Topology of AtPGAP1 (At3g27325), HsPGAP1 and Bst1p proteins as predicted by TMHMM method. Results obtained by the CCTOP web server (Dobson et al, 2015). Colours are based on the localization: blue, red and yellow for luminal, cytoplasmic and membrane regions, respectively. Triangle, lipase consensus domain.

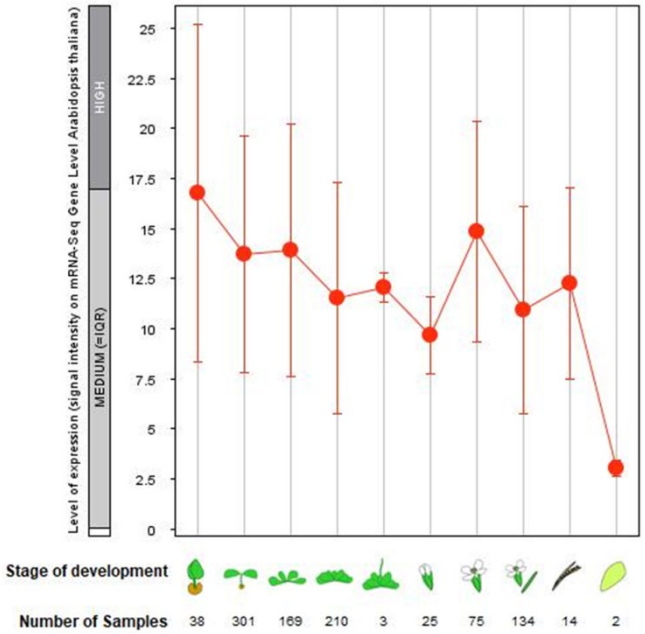

Supplemental Figure S3. Developmental expression of Arabidopsis PGAP1. Developmental stage-specific expression patterns of PGAP1. Seedlings, rosette leaves, floral organs and siliques are sequentially marked from left to right. “HIGH,” “MEDIUM,” and “LOW” expression were calculated by RNA-seq assay. The number of samples indicates RNA-seq gene expression data collected by GENEVESTIGATOR (www.genevestigator.com). Error bars represent standard deviation.

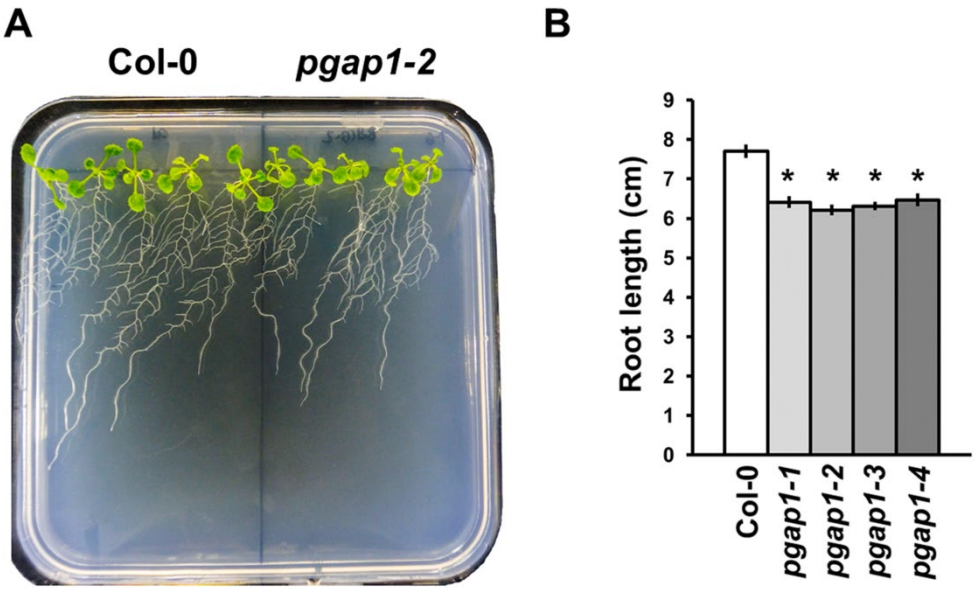

Supplemental Figure S4. Root length in *pgap1* mutants. A. 13 day-old seedlings of wild-type and *pgap1-2* mutant. B. Quantification of root length (cm) of *pgap1* mutants and wild-type 13 day-old seedlings expressed as mean $\pm$ SEM (n = 12). * statistic differences based on Student's t test with $p < 0.05$.

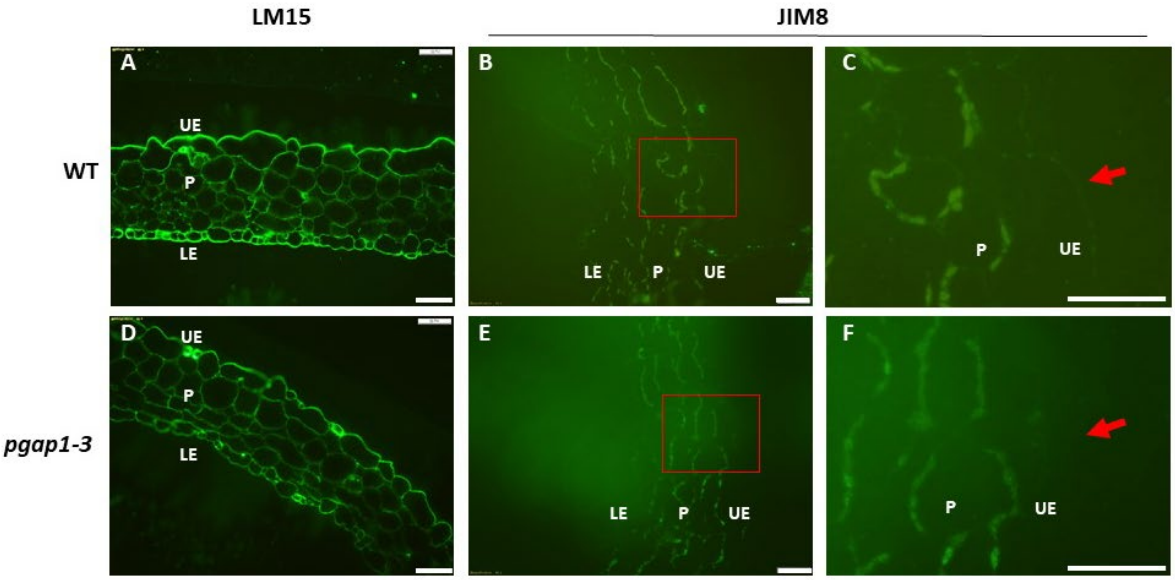

Supplemental Figure S5. Fluorescence labelling of antibodies detecting xyloglucan (LM15) and arabinogalactan-protein (JIM8) epitopes in cell walls of wild-type (Col-0) and *pgap1-3* cotyledons. LM15 signals were detected in transverse sections of wild-type (A) and *pgap1-3* (D) cotyledon walls of all cell types including upper epidermis (UE), lower epidermis (LE) and parenchyma (P). Immunofluorescence detection of arabinogalactan-protein epitopes recognized by JIM8 showed a weak signal in walls of the upper and lower epidermis of wild-type (B,C) that could not be detected in *pgap1-3* cotyledons (E,F). Boxed region in B and E shown at higher magnification in C and F with red arrows indicating walls of the upper epidermis. Scale bar = 20 µm. Images are representative of 2 biological replicates, each with 2 technical replicates

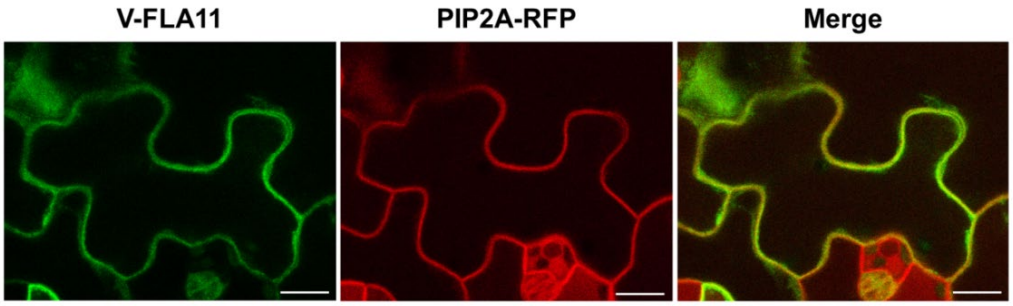

Supplemental Figure S6. Localization of V-FLA11 in wild-type (Col-0) seedlings. Transient co-expression in wild-type *Arabidopsis* seedlings of V-FLA11 (left panel) and PIP2A-RFP (medium panel) (see merged image in right panel). Scale bars = 10 μm.

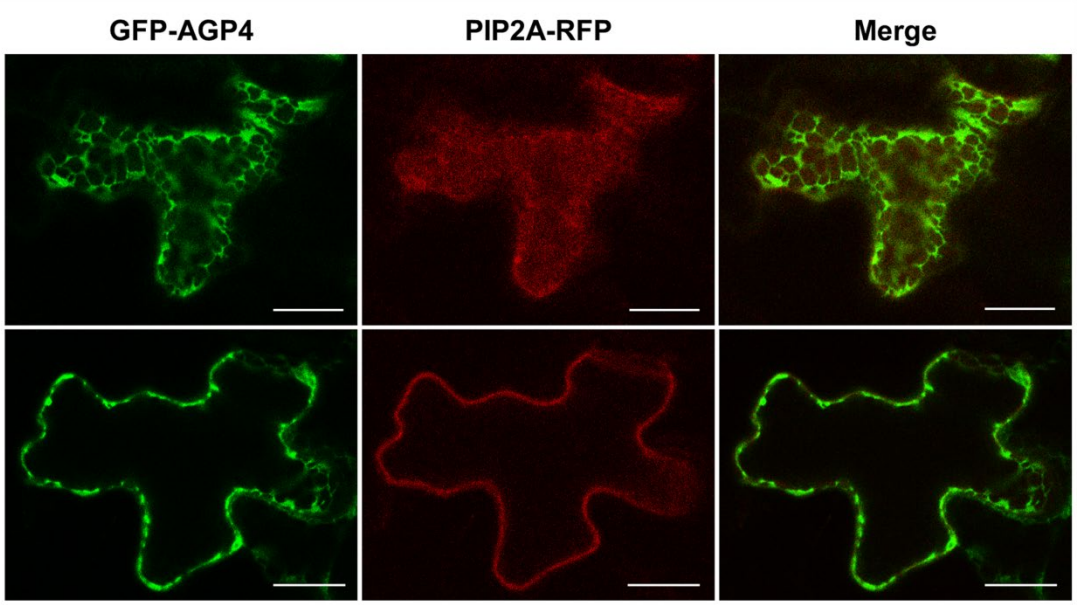

Supplemental Figure S7. Localization of GFP-AGP4 and PIP2A-RFP *pgap1-3* seedlings. Transient co-expression of GFP-AGP4 (left panels) and PIP2A-RFP (medium panels) in *pgap1-3* seedlings (see merged images in right panels). Scale bars = 10 μm.

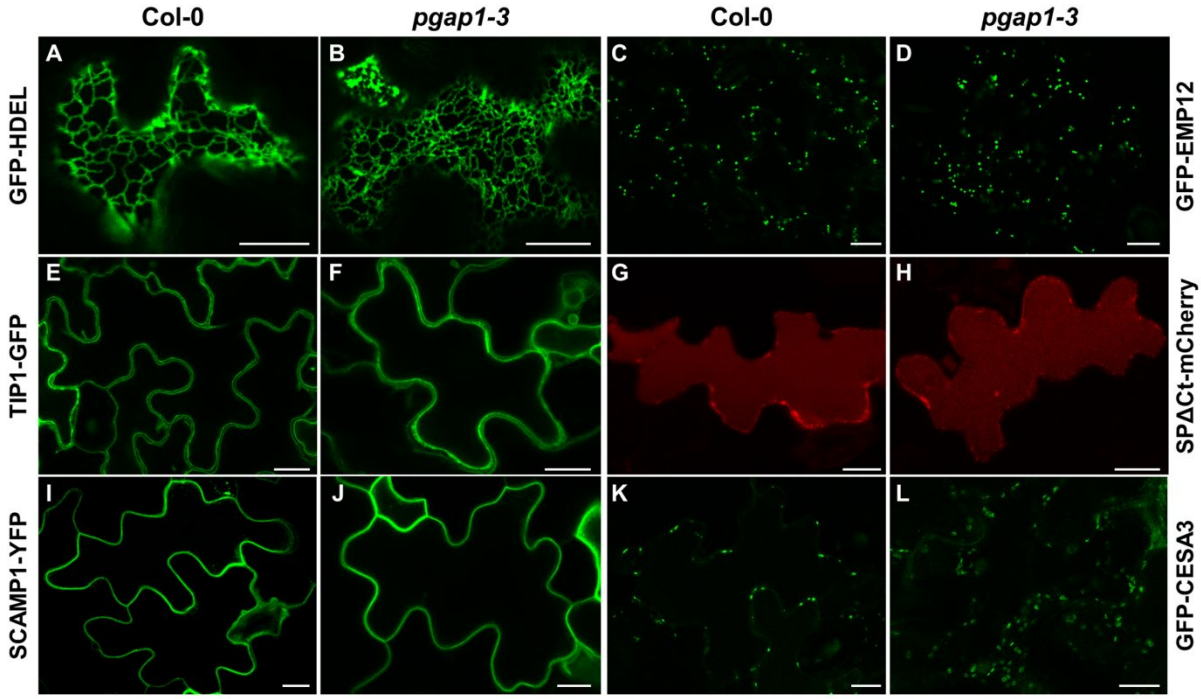

Supplemental Figure S8. Localization of organelle marker proteins in wild-type (Col-0) and *pgap1-3*. Transient expression in *Arabidopsis* seedlings of organelle marker proteins, including GFP-HDEL (endoplasmic reticulum) (A-B), GFP-EMP12 (Golgi apparatus) (C-D), TIP1.1-GFP (tonoplast) (E-F), SPΔCt-mCherry (vacuole lumen) (G-H), SCAMP1-YFP (plasma membrane) (I-J) or GFP-CESA3 (*trans* Golgi network (TGN)/plasma membrane) (K-L). Scale bars = 10 μm.

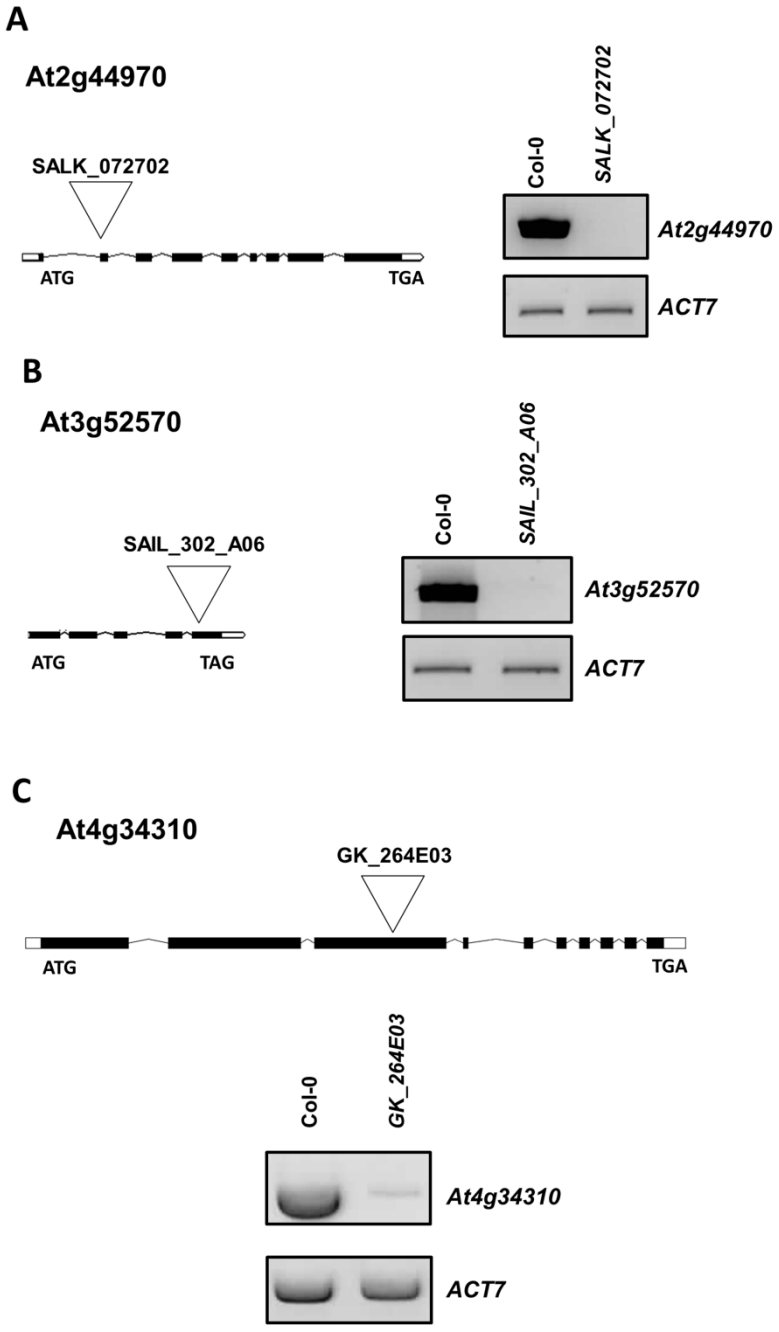

Supplemental Figure S9. Mutants in other AB_hydrolases genes different from *PGAP1*. Diagram of *At2g44970* (A), *At3g52570* (B) and *At4g34310* (C). Black boxes represent coding regions, white boxes represent 5′ UTR and 3′ UTR regions and triangles represent the localization of the T-DNA insertion in their corresponding T-DNA mutants. RT-sqPCR analysis of *At2g44970*, *At3g52570* and *At4g34310* expression in their corresponding mutants (see Supplemental tables 2 and 3 for primers) is also shown. *Actin-7* (*ACT7*) was used as a control.

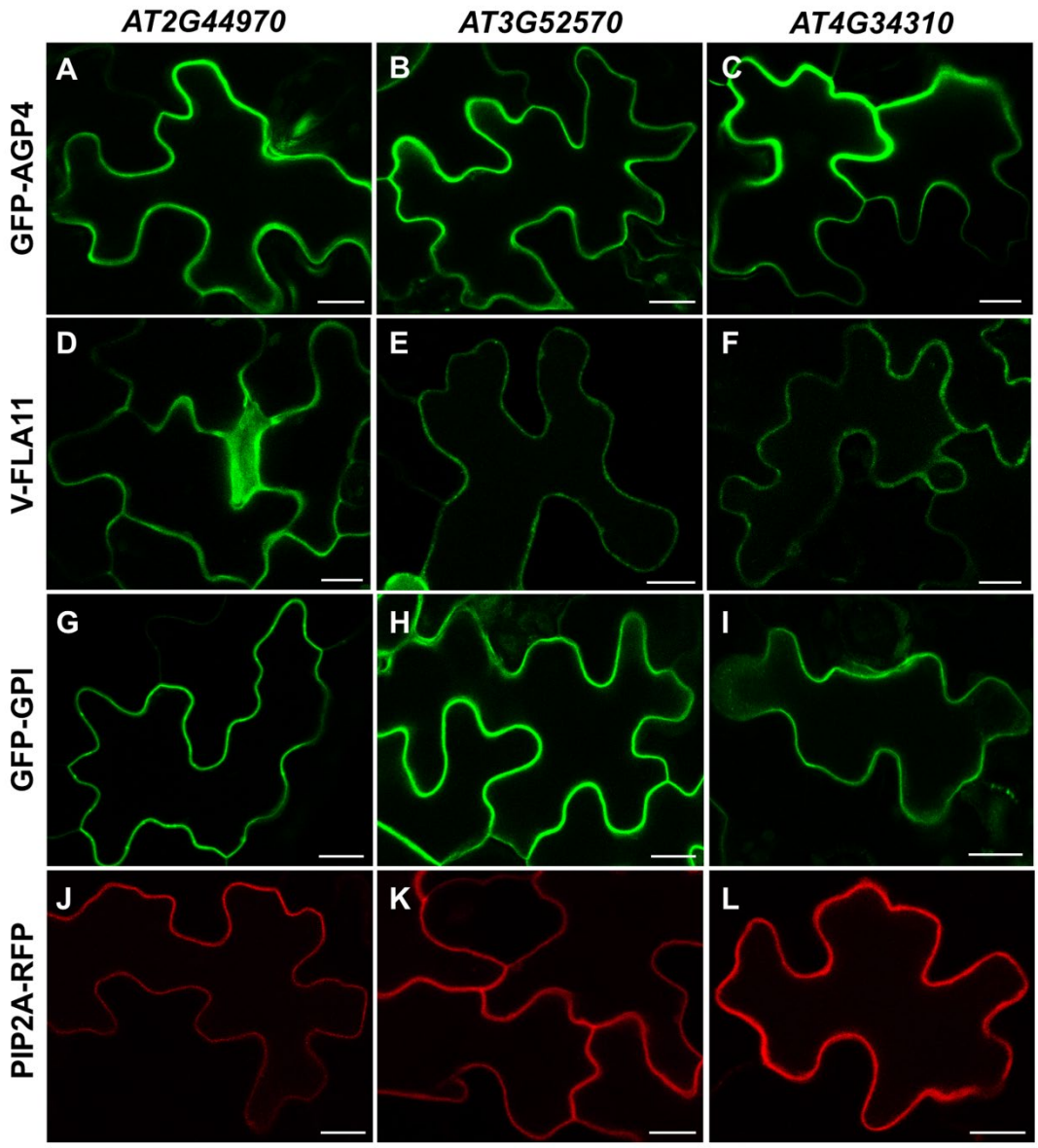

Supplemental Figure S10. Localization of plasma membrane proteins in mutants of other AB_hydrolases genes different from *PGAP1*. Transient expression in *Arabidopsis* seedlings. Three different GPI-APs, GFP-AGP4 (A-C), V-FLA11 (D-F) and GFP-GPI (G-I) mainly localized to the plasma membrane in *at2g44970*, *at3g52570* and *at4g34310* mutants, similar to the transmembrane plasma membrane protein PIP2A-RFP (J-L). Scale bars = 10 μm.

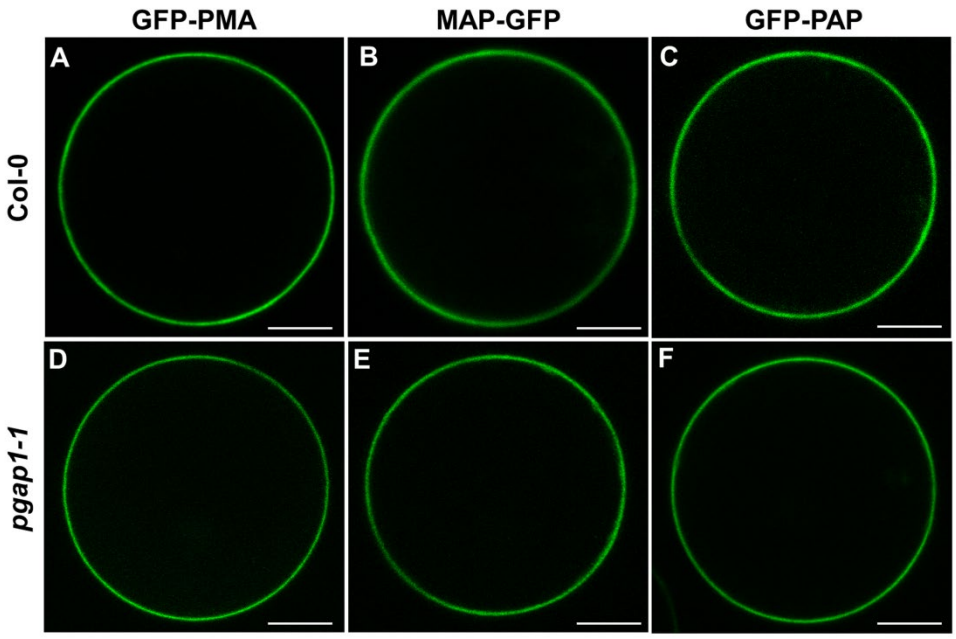

Supplemental Figure S11. Localization of plasma membrane proteins without a GPI anchor in wild-type and *pgap1-1* protoplasts. GFP-PMA (A, D), MAP-GFP (B, E) and GFP-PAP (C, F) localized mainly to the plasma membrane in protoplasts from both wild type (A to C) and *pgap1-1* mutant (D to F). Scale bars = 10 μm.

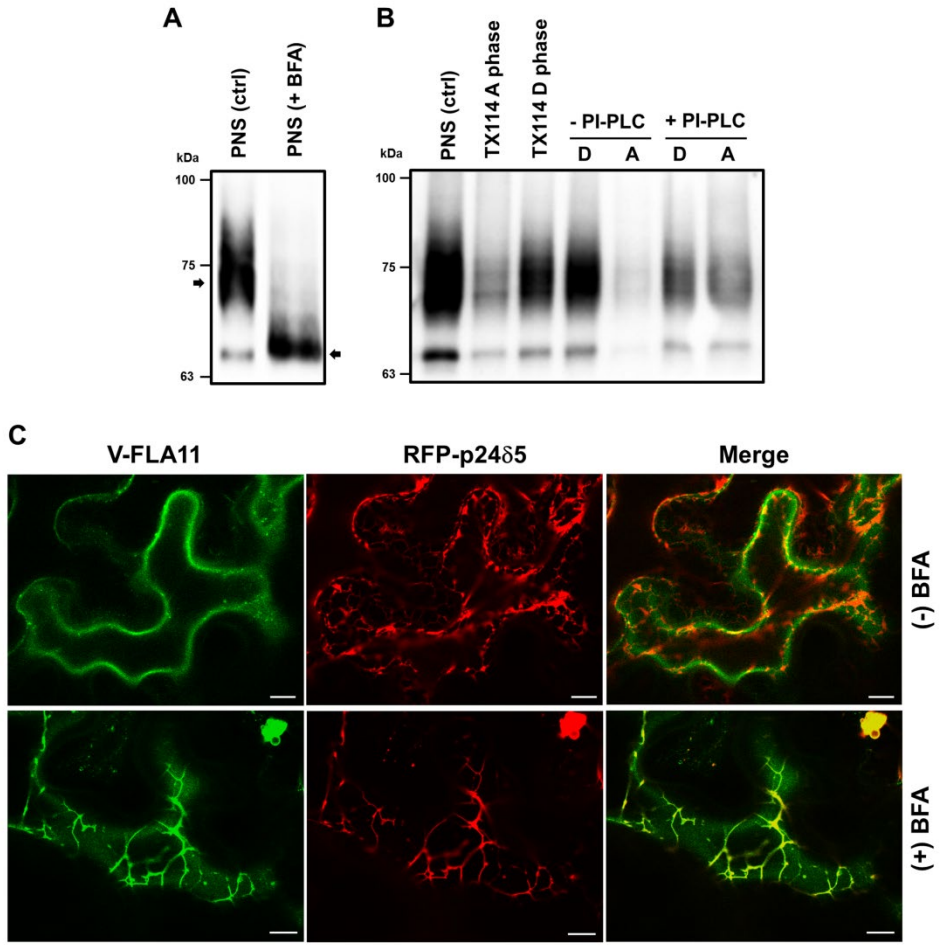

Supplemental Figure S12. Biochemical characterization of V-FLA11. A. PNSs from *N. benthamiana* leaves transiently expressing V-FLA11 and treated in the absence (PNS ctrl) or presence of BFA (PNS + BFA) were analyzed by SDS-PAGE and immunoblotting with GFP antibodies (to detect V-FLA11). Arrows show the presence of a major smear at 70-75 kDa in the absence of BFA and a 65 kDa band that was much more prominent upon BFA treatment. **B**. A PNS from *N. benthamiana* leaves expressing V-FLA11 was extracted with TX-114, and the TX-114 detergent phase was treated in the absence (-) or presence (+) of PI-PLC. After the treatment, detergent (D) and aqueous (A) phases were separated and analyzed by SDS-PAGE and immunoblotting with GFP antibodies (to detect V-FLA11). Of note, V-FLA11 mainly appears in the TX-114 detergent phase and upon PI-PLC treatment, the 70-75 kDa smear and the 65 kDa band disappeared from the detergent phase and appeared in the aqueous phase. **C**. Effect of BFA treatment on localization of V-FLA11 (left panels) and RFP-p24δ5 (medium panels) (see merged images in right panels) in *N. benthamiana* leaves. For the (+) BFA condition, leaves were infiltrated with BFA 2 d after agroinfiltration and left for an extra day before confocal laser microscopy analysis. For the (-) BFA condition, leaves were analyzed 3 d after agroinfiltration. Scale bars = 10 µm.

Table S1. **Putative *Arabidopsis* GPI inositol-deacylase *PGAP1-like* genes.** For membrane topology it was used the TMpred program, (Hofmann and Stoffel, 1993) and the data for the expected subcellular localization was obtained from TAIR (Arabidopsis.org).

	Length (aa)	**Membrane Topology**	**Expected subcellular localization**
AT2G44970	503	Transmembrane	Nucleus
AT3G29790	144	Probably not a transmembrane protein	Nucleus
AT3G27325	**1121**	**Transmembrane**	**ER/Plasma membrane**
AT3G52570	335	Probably not a transmembrane protein	Mitochondria
AT4G34310	1228	Transmembrane	Chloroplast/Mitochondria
AT5G17670	309	Probably not a transmembrane protein	Chloroplast

Table S2. **Polysaccharide calculations.** The average of two technical replicates is shown for each biological replicate.

			Col-0 A	Col-0 B	*pgap1-3* A	*pgap1-3* B
Pectic Polysaccharides						
	Arabinan	1,5-Ara (f)	3.33	3.88	6.76	4.44
		1,3,5-Ara (f)	0.47	0.99	0.82	1.09
		1,2,5-Ara (f)	0.45	0.54	0.75	0.50
		t-Ara	0.92	1.54	1.57	1.59
		Total Arabinan	**5.16**	**6.95**	**9.90**	**7.62**
	Type I AG	1,4-Gal (p)	2.63	2.32	2.68	3.21
		1,3,4-Gal (p)	0.74	1.21	0.76	0.90
		1,4,6-Gal (p)	0.11	0.15	0.21	0.26
		t-Ara	0.85	1.36	0.97	1.16
		Total Type I AG	**4.33**	**5.05**	**4.62**	**5.53**
	Type II AG	1,3-Gal (p)	0.28	0.30	0.22	0.19
		1,6-Gal (p)	1.18	0.52	0.81	0.81
		1,3,6-Gal (p)	1.41	1.47	1.00	0.90
		1,3,4,6-Gal (p)	0.05	0.00	0.03	0.05
		1,2,3,4-Gal (p)	0.18	0.20	0.00	0.05
		t-Ara	1.86	1.86	1.07	1.09
		Total Type II AG	**4.97**	**4.34**	**3.12**	**3.09**
	Homogalacturonan	1,4-Gal A /1,4-Gal A (OMe)	0.04 /0.44	0.55 /0.49	0.41 /1.23	0.59 /0.84
		t-Gal A	0.19	0.59	0.48	0.33
		Total Homogalacturonan	**0.68**	**1.63**	**2.12**	**1.76**
	RG I	1,4-Gal A	0.30	0.97	0.59	0.54
		1,2-Rha (p)	0.07	0.22	0.14	0.11
		1,2,4-Rha (p)	0.23	0.74	0.45	0.43
		Total RG I	**0.60**	**1.93**	**1.18**	**1.08**
Glucuronoxylan		1,4-Xyl (p)	4.69	4.99	3.83	4.81
		1,2,4-Xyl (p)	0.63	1.01	1.18	0.94
		t-Glc A	0.07	0.17	0.22	0.23
		Total Glucuronoxylan	**5.39**	**6.17**	**5.23**	**5.97**
Heteromannan		1,4-Man (p)	2.57	2.53	2.65	2.45
		1,4,6-Man (p)	0.42	1.01	0.90	0.86
		1,4-Glc (p)	2.57	2.53	2.65	2.45
		1,4,6-Glc (p)	0.42	1.01	0.90	0.86
		t-Gal	0.83	2.03	1.81	1.71
		Total Heteromannan	**6.80**	**9.12**	**8.92**	**8.34**
Xyloglucan		1,4,6-Glc (p)	6.09	5.61	4.21	4.45
		1,4-Glc (p)	6.09	5.61	4.21	4.45
		1,2-Xyl (p)	1.40	1.33	1.40	1.39
		1,2-Gal (p)	0.91	0.69	0.94	1.01
		t-Fuc (p)	0.91	0.69	0.87	0.94
		t-Xyl	3.23	3.60	1.94	2.11

	t-Gal	1.40	1.33	1.40	1.39
	Total Xyloglucan	**20.01**	**18.86**	**14.98**	**15.75**
Cellulose	1,4-Glc	46.68	36.23	42.33	43.90
	Total Cellulose	**46.68**	**36.23**	**42.33**	**43.90**
Callose	1,3-Glc (p)	0.12	1.17	0.40	0.65
	Total Callose	**0.12**	**1.17**	**0.40**	**0.65**
Extensin	1,2-Ara (f)	1.06	1.66	1.41	1.27
	1,3-Ara (f)	0.40	0.62	0.53	0.48
	t-Ara (f)	0.53	0.83	0.70	0.64
	t-Gal	0.13	0.21	0.18	0.16
	Total Extensin	**2.11**	**3.32**	**2.82**	**2.55**
	Total	**96.85**	**94.76**	**95.62**	**96.24**

Table S3. T-DNA mutants and PCR primers used for their characterization. Genotyping and RT-sqPCR primers used for the characterization of the mutants. Different combinations of primer pairs were used for the characterization of the mutants. The RT-sqPCR primers used in Figure 3 are in bold. RT-sqPCR analysis of *pgap1-1* showed a band of smaller molecular weight due to abnormal splicing of 14 exon due to the T-DNA insertion as detected by sequencing.

Mutant	Gene	Genotyping primers		RT-sqPCR primers
		T-DNA insertion	Wild-type allele	
SALK_072702	AT2G44970	LBb1/LPBst1A	NRPBst1A/LPBst1A	NRPBst1A/LPBst1A
SALK_078662 (*pgap1-1*)	AT3G27325	LBb1/RPBst1B	RPBst1B/LPBst1B	**RPBst1B/Bst1BR2** RPBst1B/LPBst1B Bst1BF/Bst1BR2
SAIL_1212_H07 (*pgap1-2*)	AT3G27325	LB3/LPBst1B	RPBst1B/LPBst1B	**RPBst1B/Bst1BR2** RPBst1B/LPBst1B Bst1BF/Bst1BR2
SALK_027086 (*pgap1-3*)	AT3G27325	LBb1/Bst1BF2	Bst1BF2/Bst1BR3	**Bst1BF2/Bst1BR** Bst1BF2/LPBst1B Bst1BF2/Bst1BR3
SALK_004218 (*pgap1-4*)	AT3G27325	LBb1/Bst1BR2	Bst1BF/Bst1BR2	**Bst1BF/Bst1BR2** RPBst1B/Bst1BR2
SAIL_302_406	AT3G52570	LB3/Bst1CR	Bst1CF/Bst1CR	Bst1CF/Bst1CR
GK-264E03	AT4G34310	LBG/Bst1DF	Bst1DF/Bst1DR	Bst1D/Bst1DR

Table S4. List of PCR primers used for the characterization of T-DNA mutants.

Primer	Gene	Sequence (5' → 3')	Tm (ºC)
NRPBst1A	AT2G44970	GAAACTGTCTCCTTGTGTCTATG	61
LPBst1A	AT2G44970	CTAAAGGATAAGGTCGCTGGG	61
RPBst1B	*PGAP1*	ACCAGCTTAGGTCTATTGCCC	61
LPBst1B	*PGAP1*	TTGGAAGGGAAATTTGGAAAC	55
Bst1BF	*PGAP1*	GCTCTGCAAATTGCGTTGTTTCCC	65
Bst1BF2	*PGAP1*	GGCAGCAGAATCTGATAGAGCGTT	59
Bst1BR	*PGAP1*	ACGAGACCACTGTGAAGCTTGTGAG	61
Bst1BR2	*PGAP1*	CTTTCTCTTTGATGCCATCATA	51
Bst1BR3	*PGAP1*	CAACAACTCCGGATAGTAATGGGT	57
Bst1CF	AT3G52570	ACAGCTCTCATCCTTCATGG	65
Bst1CR	AT3G52570	CCATTTTCGTAGCGCATCGT	65
Bst1DF	AT4G34310	AGCTAAAGGAGCTAGCCTACCTAA	56
Bst1DR	AT4G34310	TCCAGACCATTCCGTGAGGTTTGT	60
Housekeeping genes			
A5	*ACT-7*	GGATCCAAATGGCCGATGGTGAGG	69
A3	*ACT-7*	GGAAAACTCACCACCACGAACCAG	67
Insertion			
LBb1	T-DNA	GGATCCGCGTGGACCGCTTGCTGCAACT	76
LB3	T-DNA	TTCATAACCAATCTCGATACAC	55
LBG	T-DNA	ATATTGACCATCATACTCATTGC	51